



Title	A METHOD FOR SOLVING THE THREE DIMENSIONAL VIBRATION OF A UNIDIRECTIONAL COMPOSITE PARALLELEPIPED
Author(s)	NARITA, Yoshihiro
Citation	Materials science research international, 2(2), 105-110
Issue Date	1996-06-15
Doc URL	<a href="http://hdl.handle.net/2115/92327">http://hdl.handle.net/2115/92327</a>
Rights	©The Society of Materials Science , Japan
Rights(URL)	<a href="https://www.jstage.jst.go.jp/article/jsms1963/45/6Appendix/45_6Appendix_105/_pdf/-char/ja">https://www.jstage.jst.go.jp/article/jsms1963/45/6Appendix/45_6Appendix_105/_pdf/-char/ja</a>
Type	article (author version)
File Information	MSRI2-2_105-110.pdf



[Instructions for use](#)

Materials Science Research International, Vol.2, No.2, pp.105-110 (1996)

Publication of The Society of Materials Science, Japan

General paper

## A METHOD FOR SOLVING THE THREE-DIMENSIONAL VIBRATION OF A UNIDIRECTIONAL COMPOSITE PARALLELEPIPED

Yoshihiro NARITA

(Currently Professor Emeritus, Hokkaido University, ynarita1951@gmail.com)

Department of Mechanical Engineering, Hokkaido Institute of Technology, Sapporo, Japan

**Abstract:** A semi-analytical method is proposed for solving the free vibration problem of a rectangular parallelepiped. The parallelepiped is made of a unidirectionally reinforced fiber composite, which is modeled to have rectangular orthotropy. The method is based on the Ritz approach, and accommodates arbitrary boundary conditions on the six faces by introducing the boundary indexes into the displacement functions. Numerical results are given for the first several frequencies of isotropic and orthotropic parallelepipeds, including the cube, and are compared to the existing results obtained by other three dimensional and plate theories.

**Keywords:** *Unidirectional composite, Parallelepiped, Thick plate, Three-dimensional analysis, Ritz method, Free vibration, Natural frequency*

### 1. Introduction

Structures made of advanced composite materials are being increasingly used in many fields of engineering, mainly due to large values of specific strength and stiffness. This technical merit is obvious when compared with conventional materials, such as metals. A composite structure may be considered as an assemblage of plate and shell components, likewise in metal structures, and the vibration problem of composite plates and shells constitutes an important area in applied mechanics. A large number of analytical and experimental studies have therefore appeared on the subject in the past two decades, and some review papers have resulted, for example one written by Bert[1].

Various approximate theories for plates and shells are of course reduced from a general theory of elasticity, and from this viewpoint it is clear that accuracy of numerical results calculated by using the two-dimensional plate and shell theories must be examined by a three-dimensional analysis. In other words, the three-dimensional results serve to test the validity of a two-dimensional analysis, especially for cases where numerical difficulty is expected.

For three-dimensional vibration analysis of an isotropic parallelepiped, Fromme and Leissa[2] used the method of associated periodicity in 1970, and since then series solutions have been presented for a free or simply supported parallelepiped [3-5]. Leissa and Zhang also presented the solution procedure for a cantilevered parallelepiped in 1983 [6]. These previous studies are, however, limited to the isotropic parallelepiped with certain specific boundary conditions. For thick composite plates, some works were presented by using the first and higher order shear deformation theories [7-9], which consider approximate expressions of the displacement variation in the thickness direction.

From the reasons above, the present paper takes up a problem for which apparently no three-dimensional solutions have previously appeared, i.e., the free vibration of a unidirectional composite parallelepiped subjected to arbitrary boundary conditions on the six faces. In the analysis, the stress-strain relation is formulated by the three-dimensional theory of elasticity, and is used with the linear strain-displacement equations to derive the total potential energy. Displacements are assumed in the special series form in which the boundary indexes [10] are included. The functional (total potential energy) is extremized for stationary value with respect to unknown coefficients in the displacement functions, and a frequency equation is thus derived. Numerical results are presented for cubes and very thick plates which are comparable to results by the thick plate theories.

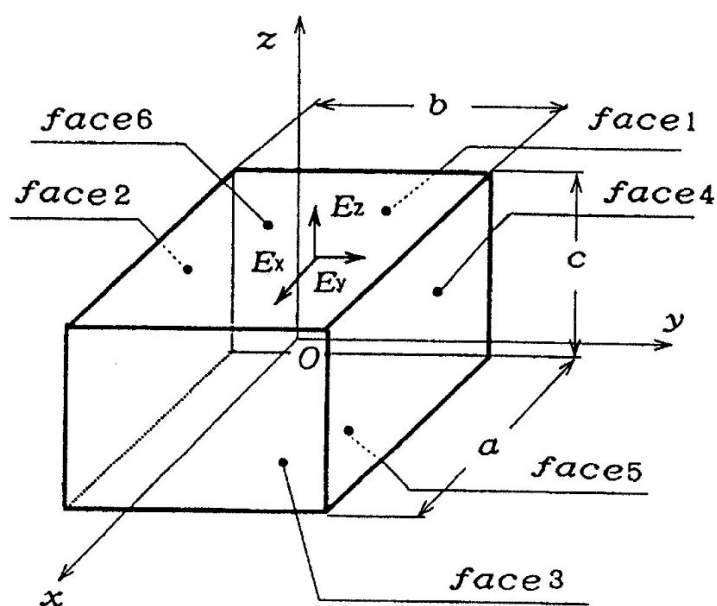


Fig. 1. Unidirectional composite parallelepiped and coordinate system.

## 2. Analytical method

As shown in Fig.1, a rectangular coordinate system  $O-xyz$  is taken so that the origin  $O$  is located in the center of the parallelepiped and the  $x$ ,  $y$  and  $z$  axes are parallel to the edges. The dimensions of

the parallelepiped are given by  $a$ ,  $b$  and  $c$  in  $x$ ,  $y$  and  $z$  directions, respectively. For material properties, the moduli of elasticity in  $x$ ,  $y$  and  $z$  directions are denoted by  $E_x$ ,  $E_y$  and  $E_z$ , respectively, and the shear moduli on the three planes are given by  $G_{xy}$ ,  $G_{yz}$  and  $G_{zx}$ . Six different Poisson's ratios are defined likewise.

Based on the macroscopic modelling, a unidirectionally reinforced composite can be modelled as an orthotropic material. In the present report dealing with specially orthotropic case, the material principal axes are assumed to coincide with  $x$ ,  $y$  and  $z$  axes, respectively, and the stress-strain relation in this case is expressed by

$$\begin{Bmatrix} \sigma_x \\ \sigma_y \\ \sigma_z \end{Bmatrix} = \begin{bmatrix} Q_{11} & Q_{12} & Q_{13} \\ & Q_{22} & Q_{23} \\ sym. & 0 & Q_{33} \end{bmatrix} \begin{Bmatrix} \varepsilon_x \\ \varepsilon_y \\ \varepsilon_z \end{Bmatrix} \quad (1)$$

$$\begin{Bmatrix} \tau_{yz} \\ \tau_{zx} \\ \tau_{xy} \end{Bmatrix} = \begin{bmatrix} Q_{44} & 0 & 0 \\ & Q_{55} & 0 \\ sym. & 0 & Q_{66} \end{bmatrix} \begin{Bmatrix} \gamma_{yz} \\ \gamma_{zx} \\ \gamma_{xy} \end{Bmatrix} \quad (2)$$

where  $Q_{ij}$  ( $i,j=1,2,\dots,6$ ) are elastic constants, defined by

$$\begin{aligned} Q_{11} &= \frac{(1 - \nu_{zy}\nu_{yz})E_x}{\Delta}, Q_{12} = \frac{(\nu_{yx} + \nu_{zx}\nu_{yz})E_x}{\Delta}, Q_{13} = \frac{(\nu_{zx} + \nu_{yx}\nu_{zy})E_x}{\Delta} \\ Q_{22} &= \frac{(1 - \nu_{zx}\nu_{xz})E_y}{\Delta}, Q_{23} = \frac{(\nu_{zy} + \nu_{zx}\nu_{xy})E_y}{\Delta}, Q_{33} = \frac{(1 - \nu_{yx}\nu_{xy})E_z}{\Delta} \\ Q_{44} &= G_{yz}, \quad Q_{55} = G_{zx}, \quad Q_{66} = G_{xy} \end{aligned} \quad (3)$$

with  $\Delta = 1 - \nu_{yz}\nu_{zx}\nu_{xy} - \nu_{yx}\nu_{xz}\nu_{zy} - \nu_{yz}\nu_{zy} - \nu_{zx}\nu_{xz} - \nu_{yx}\nu_{xy}$

The maximum displacements (amplitudes) of vibration are defined by  $u(x,y,z)$ ,  $v(x,y,z)$  and  $w(x,y,z)$  in  $x$ ,  $y$  and  $z$  directions, respectively. The strain-displacement relation is expressed by

$$\varepsilon_x = \frac{\partial u}{\partial x}, \quad \varepsilon_y = \frac{\partial v}{\partial y}, \quad \varepsilon_z = \frac{\partial w}{\partial z}, \quad \gamma_{yz} = \frac{\partial w}{\partial y} + \frac{\partial v}{\partial z}, \quad \gamma_{zx} = \frac{\partial u}{\partial z} + \frac{\partial w}{\partial x}, \quad \gamma_{xy} = \frac{\partial v}{\partial x} + \frac{\partial u}{\partial y} \quad (4)$$

From Eqs.(1),(2)and (4),the maximum strain energy stored in the parallelepiped is

$$U_{max} = \frac{1}{2} \int \{\kappa\}^T [Q] \{\kappa\} dV \quad (5)$$

where  $V$  is a volume of the parallelepiped, and  $\{\kappa\}$  is a strain vector

$$\{\kappa\} = \left\{ \frac{\partial u}{\partial x} \quad \frac{\partial v}{\partial y} \quad \frac{\partial w}{\partial z} \quad \frac{\partial w}{\partial y} + \frac{\partial v}{\partial z} \quad \frac{\partial u}{\partial z} + \frac{\partial w}{\partial x} \quad \frac{\partial v}{\partial x} + \frac{\partial u}{\partial y} \right\}^T \quad (6)$$

and  $[Q]$  is the  $6 \times 6$  matrix, where the left upper  $3 \times 3$  partitioned matrix is given by the coefficient matrix in Eq.(1) and the right lower  $3 \times 3$  matrix is by the coefficient matrix in Eq.(2).

The maximum kinetic energy is obtained as

$$T_{max} = \frac{1}{2} \rho \omega^2 \int \{u \quad v \quad w\} \begin{Bmatrix} u \\ v \\ w \end{Bmatrix} dV \quad (7)$$

where  $\omega$  is a radian frequency for free vibration and  $\rho$  is the mass density.

For simplicity in the following analytical procedure, the nondimensional quantities are introduced:

$$\xi = \frac{2x}{a}, \quad \eta = \frac{2y}{b}, \quad \delta = \frac{2z}{c}, \quad \alpha = \frac{a}{b}, \quad \beta = \frac{a}{c}, \quad (8)$$

$$\Omega = \omega a^2 \sqrt{\frac{\rho c}{D_0}}, \quad D_0 = \frac{E_y c^3}{12(1-\nu_{12}\nu_{21})}$$

There are various ways in defining a frequency parameter. For easy comparison with the plate analysis, the present parentheses defined in Eq.(8) by use of the plate bending stiffness  $D_0$ .

It is known that the Ritz method yields accurate results in the eigenvalue problem of continuous system when power series in proper form are used in the displacement functions. Then, the displacements are taken in the form

$$u(\xi, \eta, \delta) = \sum_{i=0}^I \sum_{j=0}^J \sum_{k=0}^K A_{ijk} X_i(\xi) Y_j(\eta) Z_k(\delta)$$

$$v(\xi, \eta, \delta) = \sum_{l=0}^L \sum_{m=0}^M \sum_{n=0}^N B_{lmn} X_l(\xi) Y_m(\eta) Z_n(\delta) \quad (9)$$

$$w(\xi, \eta, \delta) = \sum_{p=0}^P \sum_{q=0}^Q \sum_{r=0}^R C_{pqr} X_p(\xi) Y_q(\eta) Z_r(\delta)$$

where  $A_{ijk}$ ,  $B_{lmn}$  and  $C_{pqr}$  are unknown coefficients, and  $X$ ,  $Y$  and  $Z$  are power functions of  $\xi$ ,  $\eta$  and  $\delta$ , respectively, defined as

$$X_i(\xi) = \xi^i (\xi+1)^{B_{1u}} (\xi-1)^{B_{3u}}, \quad Y_j(\eta) = \eta^j (\eta+1)^{B_{2u}} (\eta-1)^{B_{4u}}, \quad Z_k(\delta) = \delta^k (\delta+1)^{B_{5u}} (\delta-1)^{B_{6u}}$$

$$X_l(\xi) = \xi^l (\xi+1)^{B_{1v}} (\xi-1)^{B_{3v}}, \quad Y_m(\eta) = \eta^m (\eta+1)^{B_{2v}} (\eta-1)^{B_{4v}}, \quad Z_n(\delta) = \delta^n (\delta+1)^{B_{5v}} (\delta-1)^{B_{6v}} \quad (10)$$

$$X_p(\xi) = \xi^p (\xi+1)^{B_{1w}} (\xi-1)^{B_{3w}}, \quad Y_q(\eta) = \eta^q (\eta+1)^{B_{2w}} (\eta-1)^{B_{4w}}, \quad Z_r(\delta) = \delta^r (\delta+1)^{B_{5w}} (\delta-1)^{B_{6w}}$$

In Eq.(10), the  $B_{ij}$  are "boundary indexes", which constrain the displacement functions to satisfy kinematic boundary conditions [10]. The first subscript "i" (i=1,2,...,6) in  $B_{ij}$  indicates a face of the parallelepiped under consideration, and the second subscript "j" (j=u,v,w) does the constrained displacement. For  $B_{ij}=1$ , the corresponding displacement is rigidly fixed, while it is free for  $B_{ij}=0$ . When the present analysis is applied to plate problems (i.e., for very thin solid, the upper and lower surfaces should be free), the indexes are taken as  $B_{5u}=B_{5v}=B_{5w}=B_{6u}=B_{6v}=B_{6w}=0$  and the values of other indexes along four faces (plate edges) depend upon the plate boundary conditions to be considered.

A frequency equation may be obtained in the minimization process of  $F=T_{max}-U_{max}$ , which is known as the Ritz method

$$\frac{\partial F}{\partial A_{\bar{i}\bar{j}\bar{k}}} = \frac{\partial F}{\partial B_{\bar{l}\bar{m}\bar{n}}} = \frac{\partial F}{\partial C_{\bar{p}\bar{q}\bar{r}}} = 0 \quad (11)$$

$$(\bar{i} = 0, 1, \dots, I; \bar{j} = 0, 1, \dots, J; \bar{k} = 0, 1, \dots, K; \dots)$$

and a set of homogeneous linear equations is derived as

$$\begin{bmatrix} E_{ijk\bar{i}\bar{j}\bar{k}} & E_{lmn\bar{l}\bar{m}\bar{n}} & E_{pqr\bar{p}\bar{q}\bar{r}} \\ & E_{lmn\bar{l}\bar{m}\bar{n}} & E_{pqr\bar{l}\bar{m}\bar{n}} \\ sym. & 0 & E_{pqr\bar{p}\bar{q}\bar{r}} \end{bmatrix} \begin{Bmatrix} A_{ijk} \\ B_{lmn} \\ C_{pqr} \end{Bmatrix} = 0 \quad (12)$$

An eigenvalue problem, expressed in Eq.(12), may be numerically solved by a standard subroutine. The elements in the coefficient matrix of this equation are not presented here due to the limited space.

### 3. Numerical example

By using the present three-dimensional analysis, the computation program was developed which calculate the free vibration frequencies and mode shapes for given geometric, material and constraint conditions. In the following example, the carbon fiber reinforced plastic is chosen (abbreviated as G/E), and the fiber orientation angle is taken to coincide with the  $x$  direction as in Fig.1. The elastic moduli [11] are

$$E_x=138 \text{ [GPa]}, E_y=8.96 \text{ [GPa]}, G_{xy}=7.1 \text{ [GPa]}, \nu_{xy}=0.3 \quad (13)$$

Other constants in Eq.(3) are given as

$$E_z=E_y, G_{zx}=G_{xy}, G_{yz}=E_y/[2(1+\nu_{yz})], \nu_{xz}=\nu_{xy}, \nu_{yx}=\nu_{zx}=\nu_{xy}(E_y/E_x), \nu_{yz}=\nu_{zy}=0.3 \quad (14)$$

by assuming isotropy in the  $yz$  plane. In a special case of isotropic parallelepiped, the moduli reduce to

$$E=E_x=E_y=E_z, \nu=\nu_{yz}=\nu_{zx}=\nu_{xy}=\nu_{zy}=\nu_{xz}=\nu_{yx}=0.3, G=G_{xy}=G_{yz}=G_{zx}=E/[2(1+\nu)] \quad (15)$$

In the following numerical results, the plate models are often considered for cases where the four edges are all free, simply supported or clamped. The boundary indexes used in Eq.(10) are taken, for example, in these cases as follows.

#### All edges Free

$$B_{ij}=0 \quad (i=1,2,\dots,6; j=u,v,w) \quad (\text{"}u,v \text{ and } w\text{" are free on all Faces}). \quad (16)$$

#### All edges Simply Supported

$$\begin{aligned} B_{ij}=0 \quad (i=1,3; j=u) & \quad (\text{"}u\text{" is free on Face 1 and 3}). \\ B_{ij}=1 \quad (i=1,3; j=v,w) & \quad (\text{"}v \text{ and } w\text{" are fixed on Face 1 and 3}). \\ B_{ij}=0 \quad (i=2,4; j=v) & \quad (\text{"}v\text{" is free on Face 2 and 4}). \\ B_{ij}=1 \quad (i=2,4; j=u,w) & \quad (\text{"}u \text{ and } w\text{" are fixed on Face 2 and 4}). \end{aligned} \quad (17)$$

#### All edges Clamped

$$B_{ij}=1 \quad (i=1,2,3,4; j=u,v,w) \quad (18)$$

In the all cases above, the free surface condition is necessary on the upper and lower surfaces, i.e.

$$B_{ij}=0 \quad (i=5,6; j=u,v,w) \quad (19)$$

Table 1. Convergence test for clamped plate model  
(G/E material,  $a/b=1$ ).

Number of Terms $I \times J$	$K$	5	6	7	8
<b>(a) First Frequency <math>\Omega_1</math></b>					
$a/c=1$					
$5 \times 5$	11.33	11.24	11.24	11.21	11.21
$6 \times 6$	11.33	11.24	11.24	11.21	11.21
$7 \times 7$	11.33	11.24	11.24	11.21	11.21
$8 \times 8$	11.33	11.24	11.24	11.21	11.21
$a/c=10$					
$5 \times 5$	67.76	67.75	67.75	67.75	67.75
$6 \times 6$	67.73	67.70	67.70	67.70	67.70
$7 \times 7$	67.70	67.68	67.68	67.68	67.68
$8 \times 8$	67.70	67.66	67.66	67.66	67.66
$a/c=100$					
$5 \times 5$	93.30	93.30	93.30	93.30	93.30
$6 \times 6$	93.29	93.29	93.29	93.29	93.29
$7 \times 7$	93.25	93.25	93.25	93.25	93.25
$8 \times 8$	93.24	93.24	93.24	93.24	93.24
<b>(b) Second Frequency <math>\Omega_2</math></b>					
$a/c=1$					
$5 \times 5$	14.56	14.55	14.54	14.54	14.54
$6 \times 6$	14.56	14.55	14.54	14.54	14.54
$7 \times 7$	14.56	14.55	14.54	14.54	14.54
$8 \times 8$	14.56	14.55	14.54	14.54	14.54
$a/c=10$					
$5 \times 5$	87.04	87.03	87.03	87.03	87.03
$6 \times 6$	86.69	86.67	86.67	86.67	86.67
$7 \times 7$	86.66	86.63	86.63	86.63	86.63
$8 \times 8$	86.62	86.59	86.59	86.57	86.57
$a/c=100$					
$5 \times 5$	117.1	117.1	117.1	117.1	117.1
$6 \times 6$	116.4	116.4	116.4	116.4	116.4
$7 \times 7$	116.4	116.4	116.4	116.4	116.4
$8 \times 8$	116.3	116.3	116.3	116.3	116.3

#### 4. Convergence characteristics of the solution

Because the displacement functions (9) are taken to be in series form, they must be truncated at a finite number of terms in the actual computation. Accuracy of the solution naturally depends on the number of terms, and the test for convergence rate is essential in this type of analysis.

Table 1 presents the first two frequency parameters ( $\Omega_1, \Omega_2$ ) of the clamped plate model. The planform is square ( $a=b$ ), and the thickness changes from thin plate ( $a/c=100$ ) to cube ( $a/c=1$ ). The equal number of terms are taken for each displacement (i.e.,  $I=L=P, J=M=Q, K=N=R$ ), but the number of terms  $I \times J$  in the  $x$  and  $y$  directions are independently changed with that of terms  $K$  in the  $z$  direction. It is seen for the cube ( $a/c=1$ ) that the solution is convergent for  $I \times J$  but the frequency values still decrease for  $K$ . In contrast, for thin plates ( $a/c=100$ ), the solution is still sensitive against the number of terms  $I \times J$  and is well converged for  $K$ . This convergence characteristics are understandable, because the variations in displacement through the thickness ( $z$  direction) tend to be more complicated and higher order terms are inevitably required, as the plate become thicker (i.e., approaching to a cube).

#### 5. Comparison with the plate theories

As observed in Table 1, the present method shows fast convergence rates for a wide range of the thickness ratios. This enables us to compare the present results not only with other three-dimensional results but also with those by using the two-dimensional thick plate theories. Table 2 (a) presents the first five frequency parameters of very thick isotropic plate,  $a/c=2, \nu=0.3$ ) having completely free boundaries, and compares the present results with those [9] obtained by the first-order and higher-order shear deformation theories (abbreviated as FSDT and HSDT, respectively). It is observed that the first three frequencies agree well with the HSDT values. The fourth frequency ( $\Omega_4=16.07$ ) is an in-plane (stretching) mode, which cannot be detected by the plate bending theories.

In Table 2(b), the present frequencies show excellent agreement with those obtained by the three-dimensional analysis. The plate is simply supported along the four edges, and the thickness ratio varies between  $a/c=2$  and 4.

#### 6. Exact solution for parallelepiped

It is known [6] that there are two exact solutions for free vibration of a parallelepiped. The first case is that all faces are constrained tangentially and are unconstrained normally. This means, say at a face  $x=0$  (Face 1) in Fig.1, that the displacement  $u$  is free but  $v$  and  $w$  are fixed rigidly. This boundary condition is unreal from a physical point of view, but the closed-form solution is still possible, satisfying both the equation of motion and the boundary condition exactly. The displacements in such a case are written, using nondimensional coordinates in Eq.(8), by



Table 2. Comparison of the present frequency parameters with those of (a) shear deformation plate theories and (b) three dimensional theory, for isotropic material ( $a/b=1$ ).

(a) Free Plates ( $a/c=2$ )					
	$\Omega_1$	$\Omega_2$	$\Omega_3$	$\Omega_4$	$\Omega_5$
Present	8.780	12.52	14.96	16.07	17.03
Reference [9] (by FSDT)	8.757	12.43	14.83	--	17.50
Reference [9] (by HSDT)	8.793	12.53	14.99	--	17.69

(b) Simply Supported Plate					
	$\Omega$				
$a/c$	2	2	$\sqrt{10}$	$\sqrt{10}$	4
Present	12.426	18.210	31.065	45.530	49.703
Reference [7]	12.426	18.210	31.066	45.525	49.703

Table 3. Comparison of the present frequency parameters with the exact solutions for a special case of a parallelepiped (G/E material,  $a/b=1$ ).

	$\Omega_1$	$\Omega_2$	$\Omega_3$	$\Omega_4$	$\Omega_5$
$a/c=1$					
Present	13.560	17.903	18.175	21.424	21.535
Exact ( $i,j,k$ )	13.560 (1,1,1)	17.881 (1,1,2) (1,2,1)	18.175 (1,1,1)	21.345 (1,2,2)	21.535 (2,1,1)
$a/c=2$					
Present	35.762	42.768	48.975	52.273	52.605
Exact ( $i,j,k$ )	35.762 (1,1,1)	42.689 (1,2,1)	48.975 (2,1,1)	52.231 (1,3,1)	52.274 (1,1,1)

$$\begin{aligned}
u(\xi, \eta, \delta) &= A_{ijk} \cos \frac{i\pi(\xi+1)}{2} \sin \frac{j\pi(\eta+1)}{2} \sin \frac{k\pi(\delta+1)}{2} \\
v(\xi, \eta, \delta) &= B_{ijk} \sin \frac{i\pi(\xi+1)}{2} \cos \frac{j\pi(\eta+1)}{2} \sin \frac{k\pi(\delta+1)}{2} \\
w(\xi, \eta, \delta) &= C_{ijk} \sin \frac{i\pi(\xi+1)}{2} \sin \frac{j\pi(\eta+1)}{2} \cos \frac{k\pi(\delta+1)}{2} \\
&(-1 \leq \xi, \eta, \delta \leq 1)
\end{aligned} \tag{20}$$

The second case of an exact solution is that “*sin*” and “*cos*” in Eq.(20) are interchanged, representing boundary conditions that displacements are constrained normally and unconstrained tangentially.

Although the solution (20) is useless for practical use, it can be used to verify the accuracy of approximate methods, like the Ritz method introduced here. By using Eq.(20), a frequency equation is derived, which is the  $3 \times 3$  matrix equation in terms of  $\{A_{ijk}, B_{ijk}, C_{ijk}\}$ .

Table3 presents the comparison in the frequency parameters  $\Omega$  between the exact solution and the present Ritz solution for the identical boundary conditions as in Eq.(20). The material constants for the G/E material, as shown in Eqs.(13) and (14), are used. As clearly seen from the table, two sets of frequencies show very good agreement. The  $i, j$  and  $k$  in the parentheses ( $i, j, k$ ) give the half wave number in  $x, y$  and  $z$  direction, respectively.

## 7. Effect of the thickness

Table 4 presents the first two frequency parameters  $\Omega$  of parallelepipeds having three different boundary conditions. The “F”, “S” and “C” mean that the plate boundary conditions for free, simple support and clamped edge are simulated, respectively, in the way as explained in Eqs.(16), (17) and (18). These symbols are written in counterclockwise direction for a plate planform, and for example, the CFFF denotes a cantilever (i.e., clamped at Face 1). The thickness parameter  $a/c$  is varied drastically from a cube ( $a/c=1$ ) to very thin plate ( $a/c=1000$ ).

It is observed in the table that the frequency parameters increase monotonically as  $a/c$  is increased from 1 to 1000, and show almost same values for  $a/c=100$  and 1000. The identical value  $\Omega = 4.359$  for  $\Omega_1$  and  $\Omega_2$  for CFFF indicates that one is showing a mode vibrating horizontally and the other is vibrating vertically (or vice versa). One example of such variations in the frequency parameters is shown in Fig.2, where  $\Omega$  is plotted with  $a/c$  for a clamped case (CCCC with upper and lower surfaces free). In the figure, thin straight solid flat lines are values of  $\Omega$  calculated by using CPT (Classical Plate Theory), which are not affected by the thickness explicitly. The broken lines are those obtained by FSDT. It is seen that the thick solid lines obtained by the present three-dimensional analysis gradually merge, near  $a/c=100$ , to the thin straight lines as  $a/c$  is increased, and that the FSDT values are very close to the three-dimensional results even near the cube ( $a/c=1$ ). This is observed, however, only for the lower modes and the difference is magnified for higher modes.

Table 4. Frequency parameters of parallelepipeds (from cube to thin plate) for other boundary conditions (G/E material,  $a/b=1$ ).

$a/c$	1	10	100	1000
<b>SSSS</b>				
$\Omega_1$	6.729	39.57	44.24	44.29
$\Omega_2$	8.101	58.44	67.08	67.22
<b>CFFF</b>				
$\Omega_1$	4.359	13.19	13.79	13.76
$\Omega_2$	4.359	17.12	18.58	18.61
<b>SFSF</b>				
$\Omega_1$	5.094	35.34	38.65	38.72
$\Omega_2$	7.764	38.39	43.04	43.06

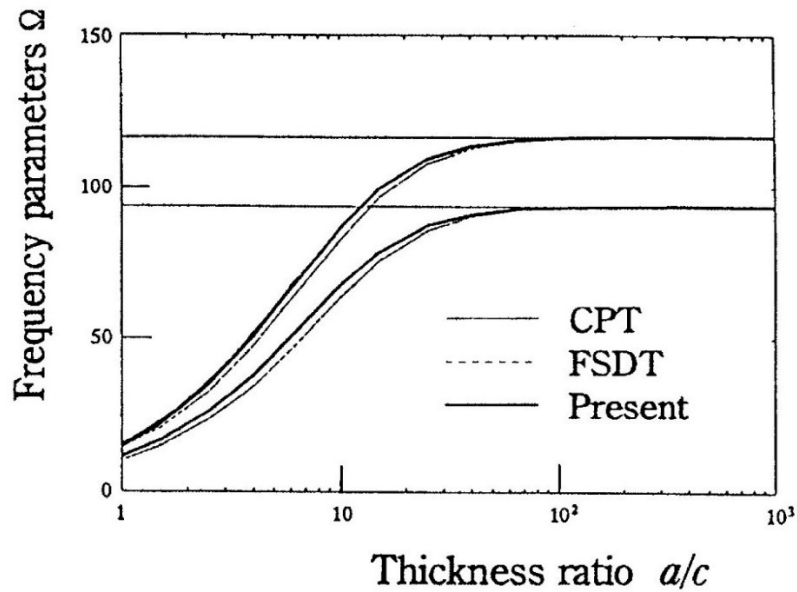


Fig.2. Variations of frequency parameters  $\Omega$  for clamped plate model (G/E material,  $a/b=1$ ).

## 8. Concluding remarks

A three-dimensional analytical method has been proposed for the solution of free vibration of a parallelepiped subjected to arbitrary boundary conditions on the six faces. First, the method was applied to the plate model where one pair of the opposite faces are free surfaces. The present results in this case were compared to those of the two-dimensional thick plate theories and of other three-dimensional theory. Secondly, an exact solution was derived to the parallelepiped with six faces constrained, and was used to compare with the present results. In all cases, the present method showed excellent agreement with other reliable data, and the validity of the method was clearly demonstrated.

## References

1. C.W. Bert, Recent Research in Composite and Sandwich Plate Dynamics, *Shock Vib. Dig.*, 11-10 (1979) 13.
2. J.A. Fromme, A.W. Leissa, Free vibration of the rectangular parallelepiped, *J. Acoust. Soc. Amer.*, 48-1 (1970) 290.
3. J.R. Hutchinson, J.R. Zillmer, Vibration of a free rectangular parallelepiped, *ASME Trans. J. Appl. Mech.*, 50 (1983) 123.
4. M. Levinson, Free vibrations of a simply supported, rectangular plate: An exact elasticity solution, *J. Sound Vibr.*, 98-2 (1985) 289.
5. E.K. Hill, The vibrational response of the rectangular parallelepiped with completely stress-free boundaries, *J. Acoust. Soc. Amer.*, 75-2, (1984) 442.
6. A.W. Leissa, Z. Zhang, On the three-dimensional vibrations of the cantilevered rectangular parallelepiped, *J. Acoust. Soc. Amer.*, 73-6 (1983) 2013.
7. S. Srinivas, C.V. Joga Rao, AK Rao, An exact analysis for vibration of simply-supported homogeneous and laminated thick rectangular plates, *J. Sound Vibr.*, 12-2 (1970) 187.
8. A.K. Noor, Free vibrations of multilayered composite plates, *AIAA J*, 11-7 (1973) 1038.
9. N.F. Hanna, A.W. Leissa, A higher order shear deformation theory for the vibration of thick plates, *J. Sound Vibr.* 170-4 (1994) 545.
10. Y. Narita, et al. Analytical method for vibration of angle-ply cylindrical shells having arbitrary edges, *AIAA J*, 30-3 (1992) 790.
11. J.R. Vinson, R.L. Sierakowski, *The Behavior of Structures Composed of Composite Materials*, Springer; First Edition (1987).